

Optimized Chemical Shift Imaging for Sodium MRI of the Human Brain

P. M. Heiler¹, B. Rieger¹, P. Krämer¹, S. Konstandin¹, and L. R. Schad¹

¹Computer Assisted Clinical Medicine, Heidelberg University, Mannheim, Germany

Introduction

Sodium MRI of the human body suffers from low sensitivity and short relaxation times. With radial projection techniques data acquisition starts in the center of k-space but echo times of 300 to 400 μ s still are in the range of the fast relaxing signal component of sodium [1]. A chemical shift imaging sequence [2] allows for quantifying the sodium concentration by fitting the FID in each voxel. During the long phase encoding, due to hardware constraints on common whole-body scanners, signal significantly decays meanwhile no data acquisition is possible. This work describes a 3D chemical shift imaging (CSI) sequence with individually minimized phase encoding durations for sodium MRI. In an additional experiment, CSI data is acquired with a Hanning weighted pre-filter [3]. Both approaches are compared to a radial projection imaging technique.

Methods

Measurements were performed on a 3 T whole-body MR system (Siemens MAGNETOM Trio, Erlangen, Germany) with a double resonant (¹H/²³Na) birdcage head coil. A phantom containing 0.9% saline solution was scanned with four different techniques.

3D-CSI: The first measurement was a generic 3D-CSI sequence with a block pulse of 0.2 ms and the following parameters: acquisition delay (half pulse duration + phase encoding duration) $T_{AD} = 0.75$ ms, repetition time $T_R = 30$ ms, readout time = 20 ms, 3 averages, FOV=200x200x120 mm³, matrix 40x40x24, resolution 5x5x5 mm³, total acquisition time T_{acq} =58 min.

3D-TE_{Min}-CSI: In the second experiment, the acquisition delay T_{AD} was reduced by individually reducing the phase encoding duration of each encoding step. Figure 1 (left) depicts this principle. Instead of a fixed gradient duration, the maximum slew rate and momentum was applied for each encoding step. Therefore, the length of the gradient differs, dependent on the k-space position, as shown in Fig. 1 (right). Minimal T_{AD} , achieved in the k-space center, is 0.1ms (half of the pulse duration). Other parameters were identical to the 3D-CSI experiment.

AW-CSI: The third CSI-scan was performed with acquisition weighted data-sampling as described in [3]. The number of averages is different in each phase encoding step in such way that measurement time and spatial resolution are not changed, compared to the previous scans.

3D-Radial: For comparison, a 3D-radial projection imaging technique was performed with identical geometrical parameters, repetition time and excitation pulse. The readout time was 20 ms and the acquisition time T_{AD} was 60 min.

In vivo Measurement: A healthy female volunteer was scanned with the 3D-AW-CSI and the 3D-TE_{Min}-CSI sequence. Identical sequence parameters were used: $T_R = 25$ ms, resolution = 6x6x6 mm³, 3 averages, $T_{ACQ} = 22$ min.

Results and Discussion:

Central slices of the phantom measurements are shown in Fig. 2. measured with the normal 3D-CSI sequence (a), the 3D-TE_{Min}-CSI sequence with minimized acquisition delay (b), the 3D-AW-CSI sequence with acquisition weighting (c) and a 3D radial projection imaging sequence (d). The optimized sequences (b,d) show higher SNR than the normal CSI sequence. In comparison to the standard 3D-CSI sequence the SNR increase is 7% for the 3D-TE_{Min} and 34% for the 3D-AW-CSI. The 3D radial projection sequence has 27% higher SNR than the 3D-CSI sequence. Additionally, the acquisition weighted sequence (c) shows less gibbs ringing artifacts than the other CSI sequences. Furthermore, blurring artifacts are diminished when compared to the radial sequence. The in vivo measurements shown in Fig. 3 demonstrate the feasibility of CSI for human brain sodium imaging in acceptable measurement time. Both approaches can be combined which should lead to a SNR increase of more than 40 % compared to the standard 3D-CSI technique.

References:

[1] Nagel et al. Magn. Reson. Med. 62:1565-1573 (2009)
[3] Pohmann R, Kienlin M. Magn. Reson. Med. 45:817-826 (2001)

[2] Brown et al. Proc. NatL Acad. Sci. USA. 79:3523-3526 (1982)

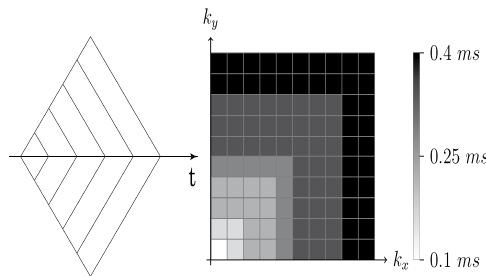


Figure 1: Phase encoding gradient of the CSI sequence with minimized acquisition delays (left). The duration of each gradient is minimized individually. Thus the acquisition delay depends on the k-space position (right).

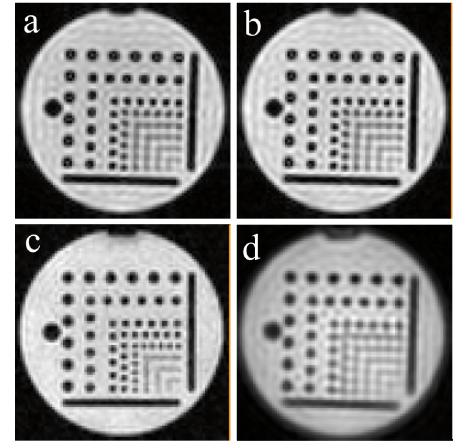


Figure 2: Central slices of a phantom containing 0.9% saline solution measured with the normal 3D-CSI sequence (a), the 3D-TE_{Min} CSI sequence with minimized acquisition delay (b), the 3D-AW-CSI sequence with acquisition weighted data acquisition (c) and a 3D radial projection imaging sequence (d).

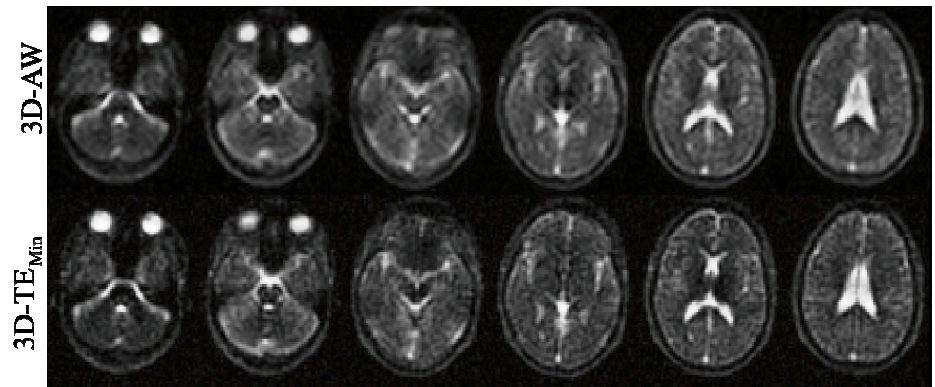


Figure 3: Axial slices, reconstructed of the 3D-datasets acquired with the 3D-AW-CSI (upper row) and the 3D-TE_{Min}-CSI (lower row) sequence.